communications medicine

Article

https://doi.org/10.1038/s43856-024-00716-3

A modeling study to define guidelines for antigen screening in schools and workplaces to mitigate COVID-19 outbreaks

Check for updates

Yong Dam Jeong[1,2,14], Keisuke Ejima[3,14] ✉, Kwang Su Kim[1,4,14], Shoya Iwanami[1], William S. Hart[5], Robin N. Thompson[6], Il Hyo Jung[2,7], Shingo Iwami[1,8,9,10,11] ✉, Marco Ajelli[12,15] & Kazuyuki Aihara[13,15]

Abstract

Background In-person interaction offers invaluable benefits to people. To guarantee safe in-person activities during a COVID-19 outbreak, effective identification of infectious individuals is essential. In this study, we aim to analyze the impact of screening with antigen tests in schools and workplaces on identifying COVID-19 infections.

Methods We assess the effectiveness of various screening test strategies with antigen tests in schools and workplaces through quantitative simulations. The primary outcome of our analyses is the proportion of infected individuals identified. The transmission process at the population level is modeled using a deterministic compartmental model. Infected individuals are identified through screening tests or symptom development. The time-varying sensitivity of antigen tests and infectiousness is determined by a viral dynamics model. Screening test strategies are characterized by the screening schedule, sensitivity of antigen tests, screening duration, timing of screening initiation, and available tests per person.

Results Here, we show that early and frequent screening is the key to maximizing the effectiveness of the screening program. For example, 44.5% (95% CI: 40.8–47.5) of infected individuals are identified by daily testing, whereas it is only 33.7% (95% CI: 30.5–37.3) when testing is performed at the end of the program duration. If high sensitivity antigen tests (Detection limit: 6.3×10^4 copies/mL) are deployed, it reaches 69.3% (95% CI: 66.5–72.5).

Conclusions High sensitivity antigen tests, high frequency screening tests, and immediate initiation of screening tests are important to safely restart educational and economic activities in-person. Our computational framework is useful for assessing screening programs by incorporating situation-specific factors.

Plain language summary

During the COVID-19 pandemic, people actively sought safer ways to resume in-person educational and economic activities while keeping the risk of infection low. For this, it may have been key to implement regular screening tests for individuals in places like schools and workplaces, since these tests can identify positive cases and help prevent the spread of the virus within these settings. Here, we introduce a computer model that evaluates the effectiveness of different screening programs in those facilities. The model involves how the virus spreads between people and within the human body, considering how the accuracy of tests can change as the infection progresses. The study examines various screening strategies. The simulations demonstrate that using highly sensitive tests, conducting frequent screenings, and starting the tests immediately are crucial for effectively identifying positive cases. Our approach can be flexibly expanded in the future to consider various factors like vaccination and new variants.

In early 2020, SARS-CoV-2, the virus responsible for COVID-19, rapidly spread throughout the world. Some of the main reasons why COVID-19 was hard to contain are its high transmissibility[1] and substantial transmission from pre-symptomatic and asymptomatic infected individuals[2–5]. While vaccines were key to dramatically decreasing COVID-19 burden[6], they only offer partial protection against infection and immunity wanes over time[7–11]. In fact, as shown by the Omicron outbreaks in China in late 2022/early 2023, COVID-19 still has the potential to put great pressure on healthcare systems[12,13]. This, coupled with the emergence of new SARS-CoV-2 variants, highlights the importance of studying mechanisms to mitigate future COVID-19 outbreaks.

The COVID-19 pandemic has changed the way we think about in-person work and education. While online working and education have become more widespread during the pandemic, they do not offer the same

A full list of affiliations appears at the end of the paper. ✉e-mail: keisuke.ejima@ntu.edu.sg; iwami.iblab@bio.nagoya-u.ac.jp

benefits as in-person interactions[14]. For example, studies have shown that the shift to online teaching has led to a decline in course completion rates among college students[15], as well as a negative impact on mental health, anxiety, and depression[15–19]. Regarding remote work, the impact on productivity is controversial and depends on types of stress (i.e., job-related and non job-related) and industries[20–23].

To guarantee a safe in-person presence in schools and workplaces, different testing and screening policies have been implemented during the pandemic with various levels of success[24]. We can summarize these policies into two main categories: symptomatic testing and mass testing. First, symptomatic testing is based on testing (e.g., through PCR or antigen tests) of individuals showing certain pre-defined symptoms (e.g., fever, respiratory symptoms); individuals with confirmed infection are then isolated (e.g., at home or in dedicated facilities) and other action may be taken (e.g., start of a contact tracing investigation, quarantine of household members, quarantine of colleagues). Second, mass testing is based on the screening of an entire population (e.g., all students at a school, all city residents) using viral tests such as PCR or antigen tests regardless of symptoms[25,26]. As for symptomatic testing, individuals who test positive are then isolated, and the policy may also entail further actions. Given the substantial fraction of asymptomatic infections[27–29] and pre-symptomatic transmission[5,30,31], epidemiological and modeling studies have shown that control strategies involving mass testing generally provide much larger mitigation effects, although they are more expensive[32–34]. However, to safeguard in-person economic and educational activities, further research is needed to define effective guidelines for the operational implementation of screening protocols.

In this study, we conduct a model-based evaluation of the effectiveness of various screening programs in schools and workplaces to determine the optimal screening schedule, screening duration, and timing of screening initiation based on the sensitivity of the adopted test. Indeed, our aim is to investigate the optimal screening programs that a facility (e.g., a firm) can self-implement to maintain its operation. Thus, we assume that the screening programs are implemented in a single facility, not multiple facilities at the same time. As a consequence, we are not interested in analyzing the effect of antigen screenings in controlling outbreaks in the community.

Methods

Overview of the model

We used computational modeling to assess the effectiveness of alternative screening programs. We developed two models working at different scales: i) a model of virus transmission between individuals in a community where the facility under screening belongs, and ii) a model of the within-host viral dynamics for each infected individual in the facility. The viral dynamics model is a compartmental model composed of two components: the amount of the virus and the proportion of uninfected target cells. The model was parameterized using longitudinal viral load data collected from over 200 SARS-CoV-2 infected individuals. The between-hosts transmission model was also a compartmental model, where the population is divided into six classes characterized by infectious status, immune status, and symptom presence.

We considered multiple screening programs, each of which was determined by five factors: (1) screening schedule, (2) sensitivity (i.e., detection limit) of the antigen test, (3) timing of screening program initiation, (4) number of available tests per person, and (5) screening duration. We only considered screening using antigen tests, because antigen tests are more realistic for screening settings given their lower cost and shorter turnaround time (time between sampling and returning results) compared to PCR tests[32]. All individuals in the facility were tested under the same schedule.

The screening programs are implemented to identify infected individuals to avoid the possibility of further spread of the infection in the facility. Thus, we set the primary and secondary outcomes of our analysis to be the proportions of infected individuals and the proportion of pre-infectious (i.e., latent) and infectious individuals identified during the screening period among all infected individuals before the screening program, respectively. It is important to note that individuals who developed symptom before screening were not counted in both the numerator and the denominator.

Note that the stochasticity lays on the viral load trajectory (the parameter sets were resampled from the estimated distributions of model parameters), measurement error of viral load, timing of infection of infected individuals in the facility, and timing of symptom onset. Results are based on 100 stochastic realizations of each analyzed scenario.

Viral load data

Longitudinal viral load data for symptomatic and asymptomatic SARS-CoV-2 infected individuals were obtained from the literature. We conducted a systematic search using PubMed and Google Scholar with the following inclusion criteria: (1) viral loads were measured and reported at least at two time points for the same patient; (2) samples were collected from upper respiratory specimens, such as nose and pharynx; (3) patients should not have received an antiviral treatment. Most of the identified studies reported cycle threshold (Ct) values, which correspond to the number of amplification cycles required to create enough copies of the viral RNA to be detected in PCR testing. As in previous studies[35,36], the viral load (copies/mL) was estimated from the Ct values using the following conversion formula: $\log_{10}\left(\text{Viralload}\left[\text{copies/mL}\right]\right) = -0.32 \times \text{Ctvalues}\left[\text{cycles}\right] + 14.11$. IRB review was exempted at Nanyang Technological University (IRB-2022–1041).

SARS-CoV-2 viral dynamics model

To describe the temporal change in viral load of each infected individual, we used an already established mathematical model describing SARS-CoV-2 viral dynamics[37–41]:

$$\begin{aligned} \frac{df(t)}{dt} &= -\beta f(t)V(t), \\ \frac{dV(t)}{dt} &= \gamma f(t)V(t) - \delta V(t), \end{aligned} \tag{1}$$

where $f(t)$ is the ratio between the number of uninfected target cells at time t (since infection) and the number of uninfected target cells at the infection time, and $V(t)$ is the amount of virus per unit of sample specimens (copies/mL) at time t. The parameters γ, β and δ represent the maximum viral replication rate, the rate constant for virus infection, and the death rate of infected cells, respectively. Time $t = 0$ corresponds to the time of infection, thus $f(0) = 1$. We assumed $V(0) = 10^{-2}$ (copies/mL)[42]. Under reasonable parameter setting, $V(t)$ increases exponentially initially, then starts declining after reaching a peak. Model parameters were estimated by fitting Eq. (1) to the longitudinal viral load data using a nonlinear mixed-effect modeling approach. The nonlinear mixed-effect model allows the estimation of population parameters while accounting for variability in parameter values between individuals[43,44]. As the time of infection was not observed directly, we estimated the timing of infection as well[38,39,45]. Model parameters were estimated for asymptomatic and symptomatic patients independently.

The calibrated model was used for simulating individual viral load trajectories for infected individuals. To account for measurement error, we also computed a measured viral load, $\hat{V}(t)$, in addition to the predicted viral load, $V(t)$[37,45]. The longitudinal true viral load for infected individual k, $V_k(t)$, was generated by running Eq. (1) with a parameter set, which was resampled from the estimated distributions of model parameters. The measured viral load for infected individual k was computed by adding an error term: $\log_{10}\hat{V}_k(t) = \log_{10}V_k(t) + \varepsilon_k$, $\varepsilon_k \sim N(0, \sigma^2)$. The variance of the error term, σ, was obtained by fitting a normal distribution to the residuals (i.e., the difference between the common logarithms of predicted viral load and measured viral load). Note that Eq. (1) was fitted to $\log_{10}V(t)$, not $V(t)$, because it is more natural to assume that the measurement error of Ct values (thus $\log_{10}V(t)$), which is directly measured in studies, follows normal distribution. The logarithm also allows us to avoid an issue with

fitting that skews towards large values in viral load data. All variables, parameters, and parameter values are summarized in Table 1.

Model of SARS-CoV-2 transmission in the community

To describe SARS-CoV-2 transmission between individuals, we developed another mathematical model. The model is a SLIR model, where the population at time t is divided into four compartments: Susceptible ($S(t)$), Latent (i.e., infected, but not yet infectious) ($L(t)$), Infectious ($I(t)$), and Removed (i.e., temporarily fully protected) ($R(t)$) (Fig. 1a). Note that each compartment is proportional to the total population which is fixed over time: $S(t)+L(t)+I(t)+R(t)=1$. Accounting for presence and absence of symptoms, $L(t)$ and $I(t)$ are separated into two groups (the subscripts a and s correspond to asymptomatic and symptomatic individuals, respectively). Newly infected cases are immediately allocated to either $L_a(t)$ or $L_s(t)$ following the asymptomatic ratio, p. Those in $L(t)$ move to $I(t)$ once they acquire infectiousness after the latent period. Those in $I(t)$ move to $R(t)$ once they lose infectiousness. Here, we assume that latent and infectious periods follow gamma distributions. Note that the sum of n independent exponential distributions $Exp(n\lambda)$ with mean $1/n\lambda$, is a gamma distribution $Gamma(n, n\lambda)$ with mean $1/\lambda$. Then, the model can be described by following ordinary differential equations:

$$
\begin{aligned}
&\frac{dS(t)}{dt} = -bS(t)\big(I_a(t)+I_s(t)\big),\\
&\frac{dL_{a,1}(t)}{dt} = pbS(t)\big(I_a(t)+I_s(t)\big) - 2\varepsilon_a L_{a,1}(t), \frac{dL_{a,2}(t)}{dt} = 2\varepsilon_a L_{a,1}(t) - 2\varepsilon_a L_{a,2}(t),\\
&\frac{dL_{s,1}(t)}{dt} = \big(1-p\big)bS(t)\big(I_a(t)+I_s(t)\big) - 2\varepsilon_s L_{s,1}(t), \frac{dL_{s,2}(t)}{dt} = 2\varepsilon_s L_{s,1}(t) - 2\varepsilon_s L_{s,2}(t)\\
&\frac{dI_{a,1}(t)}{dt} = 2\varepsilon_a L_{a,2}(t) - 2\sigma_a I_{a,1}(t), \frac{dI_{a,2}(t)}{dt} = 2\sigma_a I_{a,1}(t) - 2\sigma_a I_{a,2}(t),\\
&\frac{dI_{s,1}(t)}{dt} = 2\varepsilon_s L_{s,2}(t) - 2\sigma_s I_{s,1}(t), \frac{dI_{s,2}(t)}{dt} = 2\sigma_s I_{s,1}(t) - 2\sigma_s I_{s,2}(t),\\
&\frac{dR(t)}{dt} = 2\sigma_a I_{a,2}(t) + 2\sigma_s I_{s,2}(t),\\
&L_a(t) = L_{a,1}(t) + L_{a,2}(t), L_s(t) = L_{s,1}(t) + L_{s,2}(t),\\
&I_a(t) = I_{a,1}(t) + I_{a,2}(t),\ I_s(t) = I_{s,1}(t) + I_{s,2}(t),
\end{aligned}
\tag{2}
$$

where b is the transmission rate and p is the asymptomatic ratio. Note that $1/\varepsilon$ and $1/\sigma$ are the mean latent period and the mean infectious period with gamma distributions, respectively. The basic reproduction number of Eq. (2) can be derived: $R_e = p\frac{b}{\sigma_a} + \big(1-p\big)\frac{b}{\sigma_s}$.

Some of the parameters regulating the transmission model are informed by the viral dynamics model (Fig. 1b). Specifically, the latent period is defined as the interval between the time of infection and the time when the viral load crosses the infectiousness threshold (10^5 copies/mL), which may differ between asymptomatic and symptomatic infected individuals[46–49]. The infectious period is defined as the time interval during which the viral load is above the threshold. We estimated the values of these periods by running the viral dynamics model (i.e., Eq. (1) with 10,000 parameter sets resampled from the estimated parameter distributions. By fitting a gamma distribution to those values, we estimated the mean values, which were used to set $1/\varepsilon$ and $1/\sigma$. This process was performed for asymptomatic and symptomatic individuals independently (Supplementary Fig. 8).

The baseline of the asymptomatic ratio, p, was set at 70% since most infected cases did not present respiratory symptoms during the early stages of the COVID-19 pandemic[28]. However, it is important to acknowledge uncertainty in this value, as well as heterogeneity p between populations, which can be influenced by pharmaceutical interventions like vaccines. Currently, with high vaccination coverage, 80%-90% of infected cases are observed to be asymptomatic[27,29]. As we focus on implementing screening programs in schools and workplaces where most people are children or adults, and vaccination effectiveness and coverage are different between areas and age groups[50], we conducted sensitivity analyses encompassing a range of values of p from 20% to 90%.

Table 1 | SARS-CoV-2 viral dynamics model variables and parameters

Variables	Description		
$V(t)$	Viral load at time t (copies/mL)		
$f(t)$	The ratio between the number of uninfected cells at time t and that at time 0		
Parameter	**Description**	**Asymptomatic**	**Symptomatic**
γ	Maximum rate constant for viral replication (day^{-1})	6.06	6.81
β	Rate constant for virus infection ($[copies/mL]^{-1}day^{-1}$)	4.15×10^{-6}	9.41×10^{-7}
δ	Death rate of infected cells (day^{-1})	0.74	0.83
σ	Standard deviation of error term ($\log_{10}$[copies/mL])	1.82	1.64

The transmission rate, b, was assumed to be constant over the infectious period and set by considering the relationship between the reproduction number, R_e, and the other model parameters: $b = \frac{R_e}{p\frac{1}{\sigma_a}+(1-p)\frac{1}{\sigma_s}}$, where $1/\sigma_a$ and $1/\sigma_s$ are mean infectious periods for asymptomatic and symptomatic cases, respectively. The value of R_e depends on many factors including pathogen transmissibility, population immunity, social behavior, and deployed interventions. As such, we investigated a wide range of values of R_e, ranging from 1.5 to 5.0, as observed at various stages of the COVID-19 pandemic[51–53]. For the baseline analysis, we set $R_e = 2.0$. In our main analyses, the size of the school/workplace where the screening programs are implemented was assumed to be 1000. The timing of infection of each infected individual in the facility at time t was randomly sampled from a Poisson distribution of mean $m(t)$, where $m(t)$ corresponds to the product between the incidence rate in the community at time t and the number of individuals in the focus facility (i.e., 1000). The size of the community was set at 10 million people, substantially larger than that of focus facility. All variables, parameters, and parameter values are summarized in Table 2.

Simulation of alternative screening programs

We used the two models (i.e., Eq. (1) and Eq. (2) to evaluate the effectiveness of various screening programs. The effectiveness of the screening programs was assessed by the following outcomes: (i) proportion of infected individuals identified by the screening program, and (ii) proportion of latent (i.e., pre-infectious) and infectious individuals identified by the program. In both cases, the proportion is estimated as a fraction of individuals who were infected before the start of the program. Details on the estimation of these two outcomes are reported in Supplementary Note 1 and Supplementary Fig. 1.

Five parameters regulate the analyzed screening programs: screening schedule, sensitivity (i.e., detection limit) of antigen tests, screening duration (T), timing of screening initiation, and number of available tests per person (k). We investigated the six screening schedules (Fig. 1c). Schedule 0 involves daily screening of symptomatic students/workers only, while Schedule 1 includes screening of all students/workers on a daily basis. Schedules 2 and 3 are daily symptomatic screening with testing of all students and workers every two and three days, respectively. Schedule 4 consists of daily symptomatic screening and testing of all students and workers on the first day and last ($k-1$) days of screening duration. Finally, Schedule 5 pairs daily symptomatic screening with random testing of all students/workers (i.e., the screening of all students/workers takes place k times in days selected at random). Note that Schedules 1–5 are implemented until all available tests have been used, and these schedules also involve symptom screening.

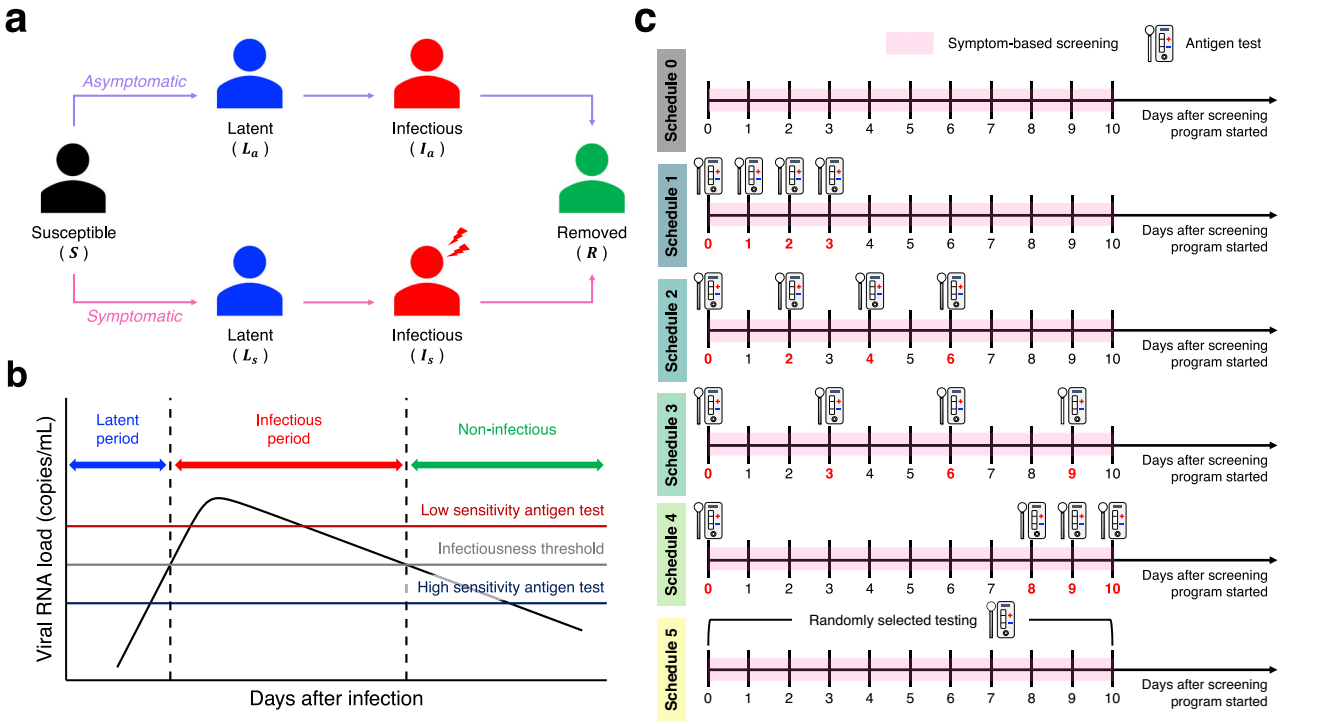

Fig. 1 | SARS-CoV-2 transmission model and viral dynamics model. a Schematic illustration of SARS-CoV-2 transmission model. **b** Three different phases of SARS-CoV-2 viral dynamics. The black solid line is a typical viral load curve (for an illustration purpose). The horizontal gray solid line is an infectiousness threshold. One goes through three phases since infection: latent (blue), infectious (red), and non-infectious (green) depending on the viral load, respectively. The horizontal red and blue solid lines are detection limits of low sensitivity and high sensitivity antigen tests, respectively. **c** Different screening schedules. The pink-shaded regions indicate a symptom-based screening. For illustration purposes, the number of antigen tests per individual is set to 4.

We assumed the screening program is implemented by a facility itself to maintain its operation. As such, the resources that the facility can decide to allocate for the screening could be highly variable. We thus assessed various scenarios. First, two antigen tests with different sensitivity were considered: low (2.0×10^6 copies/mL) and high (6.3×10^4 copies/mL)[54]. Note that the low sensitivity antigen tests are more commonly used; thus, we considered those tests in our baseline scenario. The screening duration was set as 10 days. We varied the timing of screening initiation depending on different epidemic phases: growth, peak (baseline), and decline phases (Fig. 2a). The peak phase was defined as starting on the day with the largest number of newly infected individuals in the community. The growth and decline phases are defined as starting when the number of newly infected individuals reaches 10% of the peak number of new infections (before and after the peak, respectively). The number of available tests per person was set as 4 in the baseline scenario; alternative values of 3 and 5 were explored as sensitivity analyses. The parameters of the screening programs are summarized in Supplementary Table 1. Symptom screening is triggered by symptom presence. Specifically, for each symptomatic individual, the incubation period (i.e., the period between the time of infection and onset of symptoms) was sampled from a lognormal distribution *Lognormal*(1.76, 0.41), which was estimated in our previous study[38] and gives a median incubation period of 5.8 days. It is important to stress that the incubation period does not correspond to the latent period. While the latent period is related to the transmission process (i.e., latent individuals are not yet able to transmit the infection), the incubation period is related to the clinical progression of the infection. Specifically, in this study, the incubation period plays a key role, as the onset of symptoms triggers testing.

Identified individuals are assumed to be isolated immediately. We further assume that the epidemic dynamics in the community are not affected by the dynamics in the focus school/workplace, since the size of the school or workplace is substantially smaller compared to the size of the community. Furthermore, we assume no transmission in the school/workplace as we are interested in the proportion of identified infected individuals who were infected before the initiation of the screening program.

Economic costs associated with screening programs are practically helpful to design and evaluate screening programs. To this end, we used the incremental cost-effectiveness ratio (ICER), which is defined as the ratio of the difference in costs between two strategies to the difference in effectiveness[55,56]. Here, compared to Schedule 0 (i.e., only symptom screening), we calculated the ICER of Schedules 1–5 including antigen tests (see Supplementary Note 2). We assumed the cost of rapid antigen test (i.e., lateral flow tests) is 5 USD per kit[57], although the cost could differ between countries. We did not consider the logistic costs of the program as we considered them to be similar between programs.

The statistical computing software R (version 4.2.3) was used for all analyses. A nonlinear mixed effects model analysis was performed on MONOLIX 2019R2 (www.lixoft.com). The study's supporting codes can be found on the Zenodo repository[58]. IRB review was exempted at Nanyang Technological University (IRB-2022-1041).

Reporting summary

Further information on research design is available in the Nature Portfolio Reporting Summary linked to this article.

Results

Different viral dynamics between asymptomatic and symptomatic patients

Ten papers were identified that met all the inclusion criteria. In total, the viral load data of 109 symptomatic individuals and 101 asymptomatic individuals were used to estimate the parameters of the viral dynamics model (i.e., Eq. (1). Seven studies were from Asia and two were from the USA. The other was from Europe (Supplementary Table 2).

The parameters of the viral dynamics model were fitted to the longitudinal viral load data for asymptomatic and symptomatic individuals independently (Fig. 2b and Supplementary Fig. 2). We observed differences

Table 2 | SARS-CoV-2 transmission model variables and parameters

Variables	Description		
$S(t)$	Proportion of susceptible population at time t		
$L_a(t)$	Proportion of asymptomatic latent population at time t		
$L_s(t)$	Proportion of symptomatic latent population at time t		
$I_a(t)$	Proportion of asymptomatic infectious population at time t		
$I_s(t)$	Proportion of symptomatic infectious population at time t		
$R(t)$	Proportion of removed population at time t		
Parameter	**Description**	**Baseline**	**Range**
R_e	Basic reproduction number	2.0	1.5 to 5.0
b	Transmission rate (day^{-1})	Theoretically derived*	Theoretically derived
p	Asymptomatic ratio	0.7	0.2 to 0.9
$1/\epsilon_a$	Mean latent period for asymptomatic infected individuals, modeled as a gamma distribution (day)	2.7[&]	–
$1/\epsilon_s$	Mean latent period for symptomatic infected individuals, modeled as a gamma distribution (day)	3.2[&]	–
$1/\sigma_a$	Mean infectious period for asymptomatic infected individuals, modeled as a gamma distribution (day)	6.0[&]	–
$1/\sigma_s$	Mean infectious period for symptomatic infected individuals, modeled as a gamma distribution (day)	7.4[&]	–

[&] Obtained from the viral dynamics model Eq. (1).

*$b = \frac{R_e}{\left(p\frac{1}{\sigma_a}+(1-p)\frac{1}{\sigma_s}\right)}$.

in the peak viral load and the duration of viral shedding between two groups, but not in the time of the peak viral load (Fig. 2b). The epidemiological parameters related to disease progression (i.e., the latent period and infectious period for asymptomatic and symptomatic individuals, respectively), informed by the viral dynamics model, are summarized in Table 2.

Effectiveness of screening programs

Incorporating the viral load dynamics in the transmission model (i.e., Eq. (2)), we evaluated the effectiveness of screening programs. Under our baseline epidemiological parameter setting ($R_e = 2.0$, $p = 0.7$), the daily incidence in the community peaks on epidemic day 152 and is at 10% of the peak incidence on epidemic days 116 and 187 (Fig. 2a) – we considered screening programs starting on these three days (denoted peak, growth, and decline phases of the epidemic, respectively). Assuming that the infection risk for those at the school and the workplace is dependent on that of the community, the epidemic curve at the facility is proportional to that of the community (Fig. 2a). In the growth phase, higher proportions of infected individuals are either latent or infectious because not much time has passed since their infection, whereas more individuals are already non-infectious with low viral load in the decline phase (Fig. 2a).

The effectiveness of different screening programs was assessed based on the proportion of infected individuals identified through either antigen test screening or symptom presence. We considered our baseline scenario unless otherwise specified (Table 2 for transmission model parameters and Supplementary Table 1 for screening programs). When screening tests were not performed (Schedule 0), individuals can be identified only by symptom screening during the period of the screening program (Fig. 1c). The proportion of identified individuals increases over time but saturates around Day 7, because the viral load of asymptomatic individuals who were infected before the screening program drops below the detection limit by this time (thus they cannot be identified), and symptomatic individuals who were infected before the screening program have already presented symptoms by this time. This proportion reaches 14.6% (95% CI: 13.0–16.3) by the end of the program (Schedule 0). When screening tests were performed (Schedule 1 to 5), the proportion of identified individuals after the program was remarkably higher compared with that under Schedule 0 (Fig. 2c).

Compared with other schedules, early and frequent screening (such as Schedules 1 and 2) identified more infected individuals on average (Fig. 3). In particular, 36.9% (95% CI: 33.7–40.1) and 36.0% (95% CI: 32.7–39.8) of individuals were identified by antigen tests under Schedule 1 and 2, respectively, whereas the proportion was 22.0% (95% CI: 18.9–25.6) under Schedule 4 (late screening). Also, Schedule 1 identified 7.5% (95% CI: 5.1–9.9) of symptomatic individuals with antigen testing sooner, before the onset of symptoms, compared to Schedule 0. At the peak of the epidemic, the infection stage of individuals was mainly distributed in the early stage of viral progression, which implies that their viral loads may be as high as the detection limit (Supplementary Fig. 9a). Thus, Schedule 1 effectively identified positive individuals more than other schedules.

In addition, we examined the difference in the number of used antigen tests during screening between schedules. While Schedule 1 identified individuals by using antigen tests up to 4 times properly, most individuals were identified by the first antigen test under Schedule 4 (Fig. 4a). Additionally, since Schedule 4 uses antigen tests later in the screening period, more symptomatic individuals were identified by symptom screening than by antigen tests, and thus most identified symptomatic individuals used the test only once. On the other hand, because the timing of using antigen tests in Schedule 1 is focused on earlier during the screening, most symptomatic individuals used all 4 times tests before being identified by symptom screening (Fig. 4b). We also computed the ICER of the screening programs (Fig. 4c). The ICER under Schedule 1 was estimated to be about 50, meaning that an average of 50 USD is required to identify one additional infected individual relative to Schedule 0. In contrast, Schedule 4 is estimated to require about 80 USD per additional identified infected individual compared to Schedule 0.

We varied the reproduction number (R_e) and proportion of asymptomatic infections (p). The proportion of identified individuals was negatively associated with p, because symptom screening works better for small p. Meanwhile, it was positively associated with R_e, because more individuals have a high viral load when the screening programs start as the epidemic curve gets steeper (first column panels in Fig. 5 and Supplementary Fig. 9b). Comparing the schedules under our baseline epidemiological parameter setting (Fig. 2c), Schedules 1 and 2 identified more positive individuals because their viral load was still high when they were tested. Indeed, Schedule 1 (daily screening) yielded 47.1% (95% CI: 44.2–51.0) in identifying infected individuals, whereas it was 33.7% (95% CI: 30.5–37.3) for Schedule 4 (late screening). The proportion of identified individuals by only antigen tests was also positively associated with R_e, and Schedules 1 and 2 showed better outcomes (second column panels in Fig. 5). Moreover, compared to Schedule 0 (only symptom screening), the proportion of identified symptomatic individuals by antigen tests before their symptoms have shown increased, as p decreased. Generally, symptom screening works better when there are many symptomatic patients, so in this case, there may

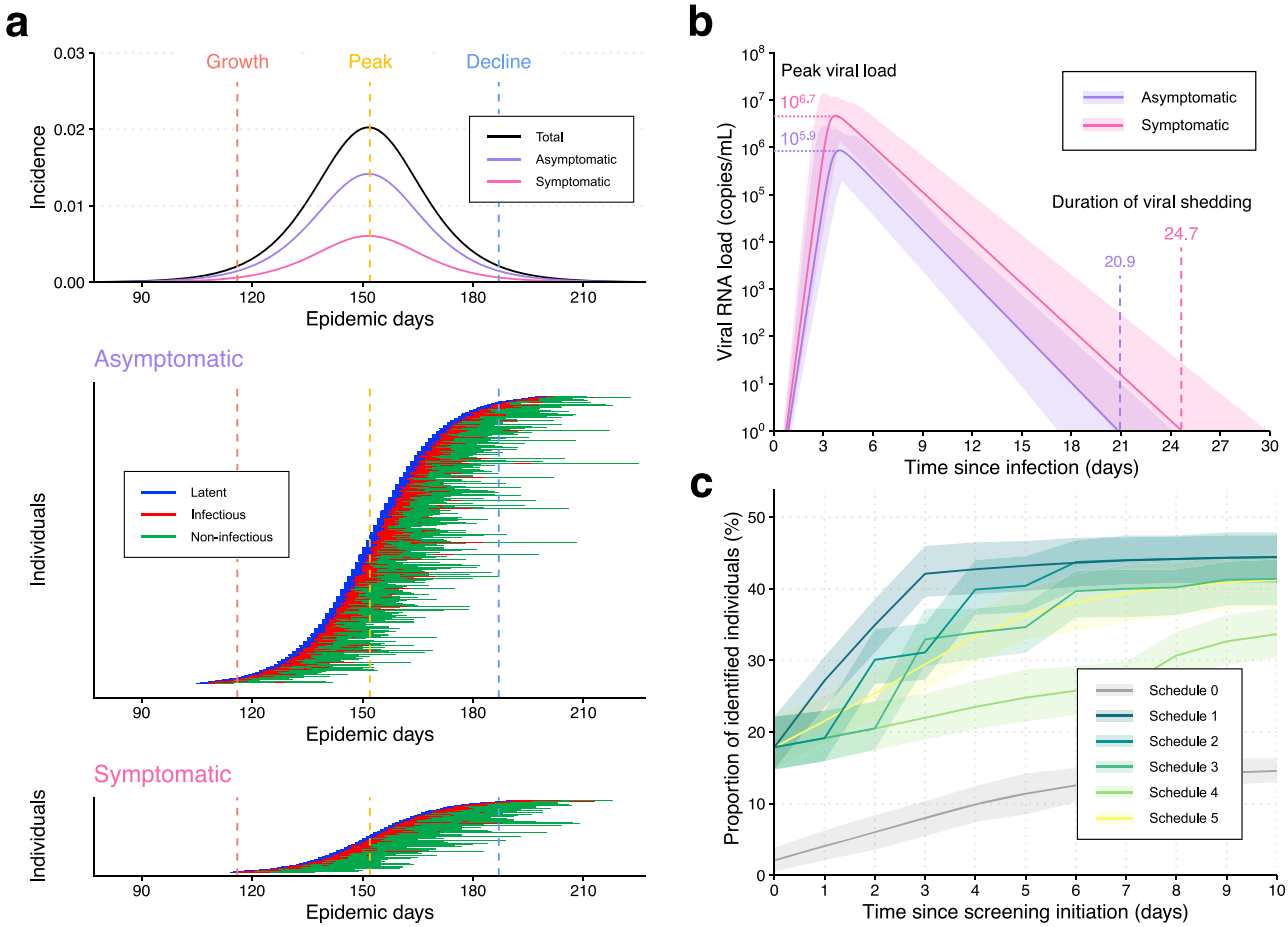

Fig. 2 | SARS-CoV-2 epidemic curves and viral load curves. a SARS-CoV-2 epidemic curves (upper panel). The black, purple, and pink curves are the daily incidence (as a proportion of the total population) of new infections, asymptomatic infections, and symptomatic infections, respectively. The vertical red, yellow, and blue dashed lines are the timings of screening initiation for the growth, peak, and decline phases of the epidemic, respectively. Simulated SARS-CoV-2 viral dynamics of asymptomatic and symptomatic individuals in the school or workplace over time (lower panel). The blue, red, and green lines are latent, infectious, and non-infectious stages as defined in Fig.1a. Note that the green line is discontinued on the right end when the viral load drops below a detection limit of 10^2 copies/mL. **b** Estimated viral load curves from the SARS-CoV-2 viral dynamics model. The solid lines are drawn using the best-fit population parameters (purple: asymptomatic, pink: symptomatic). The shaded regions correspond to 95% predictive intervals created using a bootstrap approach. **c**. Cumulative proportion of identified SARS-CoV-2 infected individuals during the screening programs (Schedules 0 to 5) under our baseline setting ($R_e = 2.0, p = 0.7$). We used baseline values for screening programs (i.e., low sensitivity tests [2.0×10^6 copies/mL], screening initiation at peak phase, and 4 antigen tests for each person). The shaded regions are 95% confidence intervals using a bootstrap approach.

be little difference in the proportion between Schedule 0 and other schedules that use antigen tests. However, since the viral load of symptomatic individuals is higher than that of asymptomatic individuals, screening using antigen tests is effective in identifying symptomatic individuals before being identified by symptom screening, even for small p (Fig. 2b and third column panels in Fig. 5).

We further explored the impact of changing the other parameters of screening programs. Higher sensitivity antigen tests, screening initiated at an earlier phase of the epidemic, and more screening tests are associated with effective screening programs (Fig. 6). Notably, 69.3% (95% CI: 66.5–72.5) of infected individuals were identified by high sensitivity antigen tests (6.3×10^4 copies/mL) under the baseline epidemiological parameter setting (Fig. 6a). The number of tests improved the effectiveness; however, the impact was minor compared with the other parameters because most of identified individuals were identified at the first few tests (Fig. 6c and Fig. 2c). In schools, screening programs tailored for young individuals may be needed. In fact, most children infected with SARS-CoV-2 remain asymptomatic[59] and have lower viral loads and shorter viral shedding than symptomatic individuals or older adults[60,61]. Therefore, antigen tests with high sensitivity may be instrumental enhance screening programs in schools. We also varied the facility size considering 500 and 2,000 as sensitivity analyses as compared with the default size of 1000. We found that the average outcomes did not depend on the size of the facility. However, the variance of the outcomes increased when the facility size decreased (Supplementary Fig. 7).

Furthermore, we repeated our analyses using the secondary outcome (the proportion of identified latent and infectious individuals) because these individuals are the source of transmission. In other words, we excluded those who had already lost infectiousness. We found quantitatively similar results as in the analyses for the primary outcome (Supplementary Fig. 3 and Supplementary Figs. 5–6). However, the ICER for the secondary outcome was slightly higher than for the primary outcome – the higher costs were entailed in specifically identifying a latent and infectious individual (Supplementary Fig. 4c). Moreover, the difference in the screening effectiveness between Schedules 1 and 4 was slightly more emphasized: the differences were about 10.2% and 12.6% for the primary and secondary outcomes on average, respectively, because more non-infectious individuals were identified by late screening (Schedule 4).

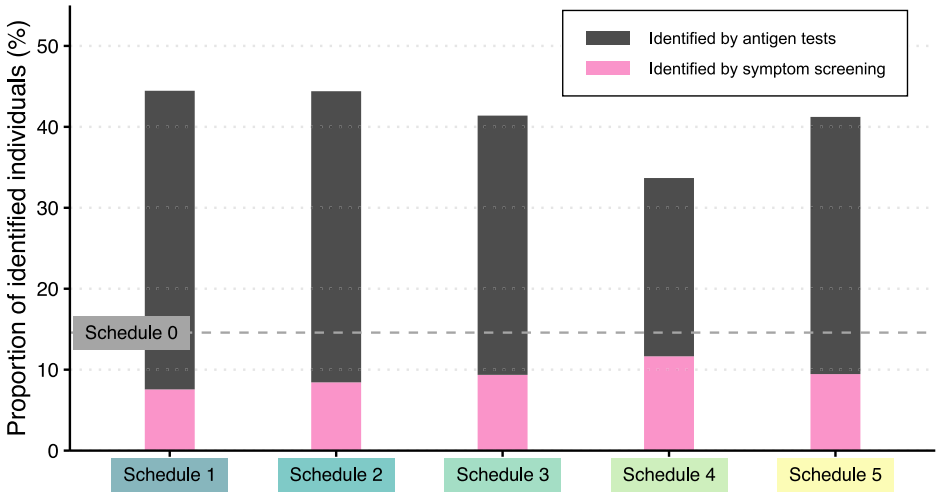

Fig. 3 | Effectiveness of different screening schedules on identifying SARS-CoV-2 infected individuals under baseline setting ($R_e = 2.0$, $p = 0.7$). Mean cumulative proportion of SARS-CoV-2 infected individuals by the end of screening programs. We used baseline values for screening programs (i.e., low sensitivity tests [2.0×10^6 copies/mL], screening initiation at peak phase, and 4 antigen tests for each person). The black and pink bars represent identified individuals by antigen tests and symptom screening, respectively. The gray horizontal dashed line means Schedule 0.

Discussion

As well as the devastating public health impacts of COVID-19, the pandemic has had substantial socio-economic costs. In countries worldwide, strategies have been sought to safely restart economic and educational activities involving in-person interactions. Screening for infection is considered as key to mitigating the risk of infection while allowing in-person interactions. We assessed the effectiveness of different screening programs using antigen tests through simulation of a multi-scale epidemiological modeling framework.

In the simulations, the transmission model and the viral dynamics model were combined to incorporate both epidemiological dynamics and within-person virological dynamics, because both factors influence the assessment of the effectiveness of screening programs. To parameterize the viral dynamics model, we used longitudinal viral load data. Further, epidemiological parameters related to disease progression (i.e., latent period and infectious periods) were informed by the viral dynamics model and used to develop the transmission model. The effectiveness of different screening programs was assessed, and sensitivity analyses were conducted in which model parameters were varied. We found that early and frequent screening with high sensitivity antigen tests yielded high effectiveness because more individuals are identified while their viral load is high. The analyses using the secondary outcomes revealed that the importance of early screening tests was emphasized when only latent and infectious individuals were counted because those individuals can only be identified when their viral load is high. This is the first study that assessed the effectiveness of screening programs with antigen tests in schools or workplaces using a multi-scale model. A previous study examined the effectiveness of screening programs targeting an entire population using a viral kinetic model and suggested that frequent screening tests with a fast turnaround time are key to mitigating the transmission risk in the population[32]. Our study is different as we focused on a small group (i.e., a school or a workplace) as the screening target, not an entire population, and the multi-scale epidemiological model was employed. Population-wide screening is feasible in an emergency. Indeed, population-wide screening was conducted in Slovakia in late 2020 and successfully controlled the epidemic at least for a short time while screening was performed[62]. Meanwhile, small-scale screening will not be powerful enough to control the epidemic at population scale. Therefore, the effectiveness of screening in a school or a workplace is influenced by the transmission risk in the population, but a smaller effect might be expected in the other direction. Further, Larremore et al. assumed screening tests are performed until the epidemic is contained[32], whereas we assumed a limited screening period. Although antigen screening is less expensive than PCR testing, enforcing all people to get tested over the pandemic period might be challenging. Further, previous studies assessed the efficacy of screening programs without using multi-scale models. For example, Leng et al. assessed the effectiveness of antigen testing in English secondary schools using an individual-based modeling[25]. The authors assumed that the sensitivity of antigen testing dynamically changed over the course of infection according to results from an epidemiological study[63]. Compared with these previous studies, test sensitivity is directly informed by the viral load in our analysis, thus we can estimate the sensitivity for different antigen tests with different detection limits, which enables us to choose appropriate antigen tests. Indeed, we found that rapid antigen tests should be designed to have lower detection limits than infectiousness threshold value in the context of isolation guideline[45].

In this study, we considered antigen tests rather than PCR testing, because using PCR testing for screening purpose is practically challenging given the cost and turnaround time (which is around 2 days[32]). There are multiple antigen tests with varying sensitivity[54]. We found that high sensitivity antigen tests available so far yielded about 18% more identified infected individuals than low sensitivity antigen tests (Fig. 5). The viral dynamics were utilized to inform both the time-dependent test sensitivity and epidemiological parameters, such as the latent and infectious periods. However, the time-dependent transmission probability was not considered in this simulation. Several studies have assumed a dynamical transmission probability informed by the viral dynamics model[49,64,65]. Nevertheless, connecting the transmission rate and viral load has been proven to be challenging, and the aforementioned studies have relied on several untestable assumptions. One direct approach to investigate the association between viral load and transmissibility involves measuring culturability depending on viral load[46,66–69]. However, culturability serves as a necessary condition for transmission but not a sufficient one, as transmission occurs not only with a culturable virus but also requires exposure to the virus, a factor not considered in culturability assessments. Another strategy involves estimating the viral load at the time of infection using viral dynamics models and information from infector-infectee pairs with longitudinal viral load data[70]. Unfortunately, such data are extremely rare, particularly during a pandemic. Furthermore, it is essential to note that the primary focus of this study is a broad assessment of the effectiveness of antigen screening, rather than a detailed modeling of transmission dynamics. For these reasons, we did not incorporate viral load information to inform a time-dependent transmission rate in our model.

We assumed the screening is triggered by the epidemic phases determined by the incidence rate. When considering an entire epidemic, the temporal dynamics of the incidence curve may follow more complex patterns with multiple waves, which do not allow for a simple definition of growth, peak, and decline phases. However, in the short-term, these three phases are generally well-defined. Nonetheless, further research is warranted to explore the effect of complex temporal epidemic dynamics on the definition of screening strategies. Although we carefully developed the

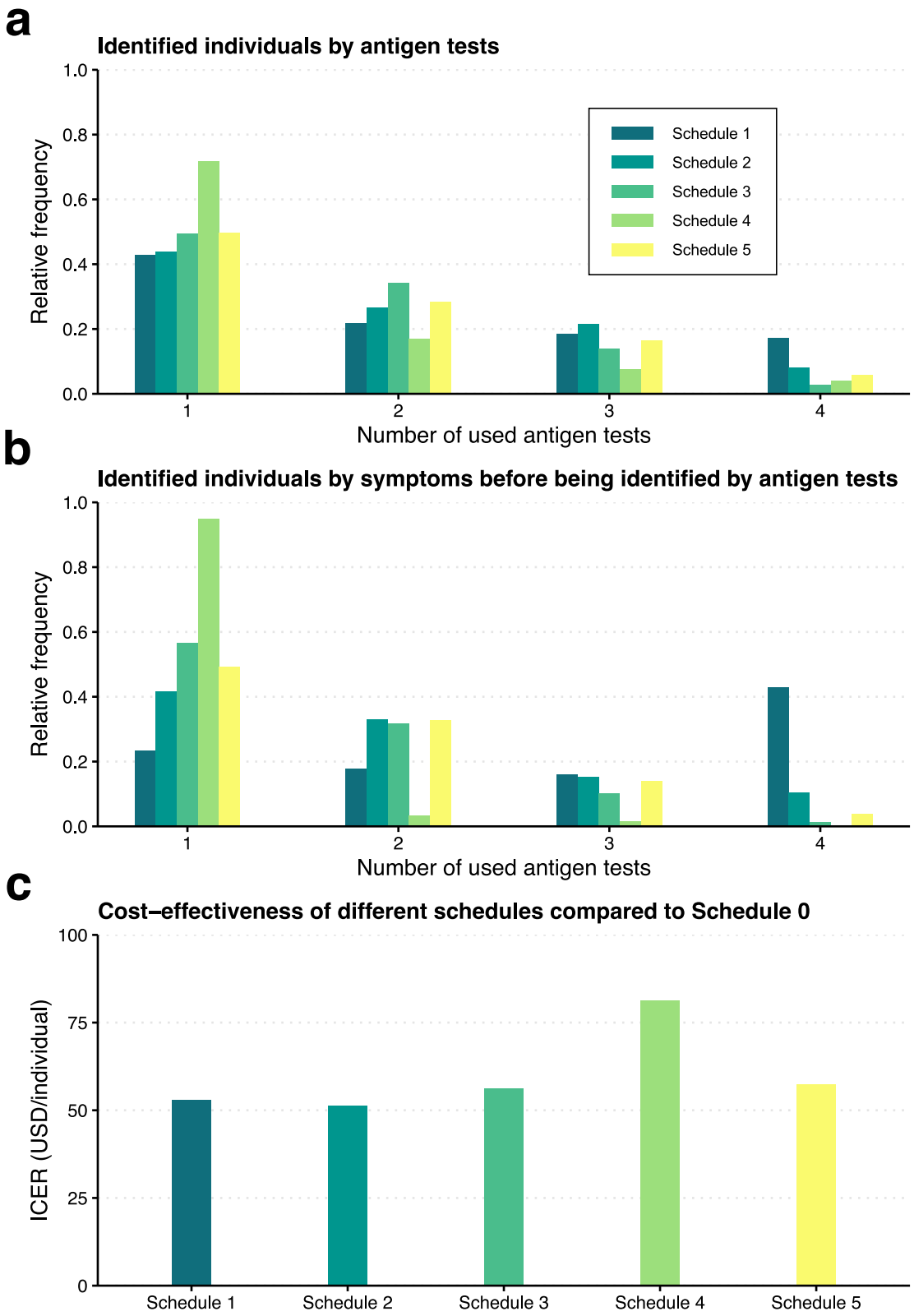

Fig. 4 | Cost-effectiveness of different screening schedules on identifying SARS-CoV-2 infected individuals under baseline setting ($R_e = 2.0, p = 0.7$). **a**. Number of used antigen tests for identifying SARS-CoV-2 infected individuals under different screening schedules. **b**. Number of used antigen tests for identifying SARS-CoV-2 symptomatic individuals before being identified by antigen tests under different screening schedules. **c**. Incremental cost-effectiveness ratio (ICER) of different screening schedules compared to Schedule 0. We used baseline values for screening programs (i.e., low sensitivity tests [2.0×10^6 copies/mL], screening initiation at peak phase, and 4 antigen tests for each person).

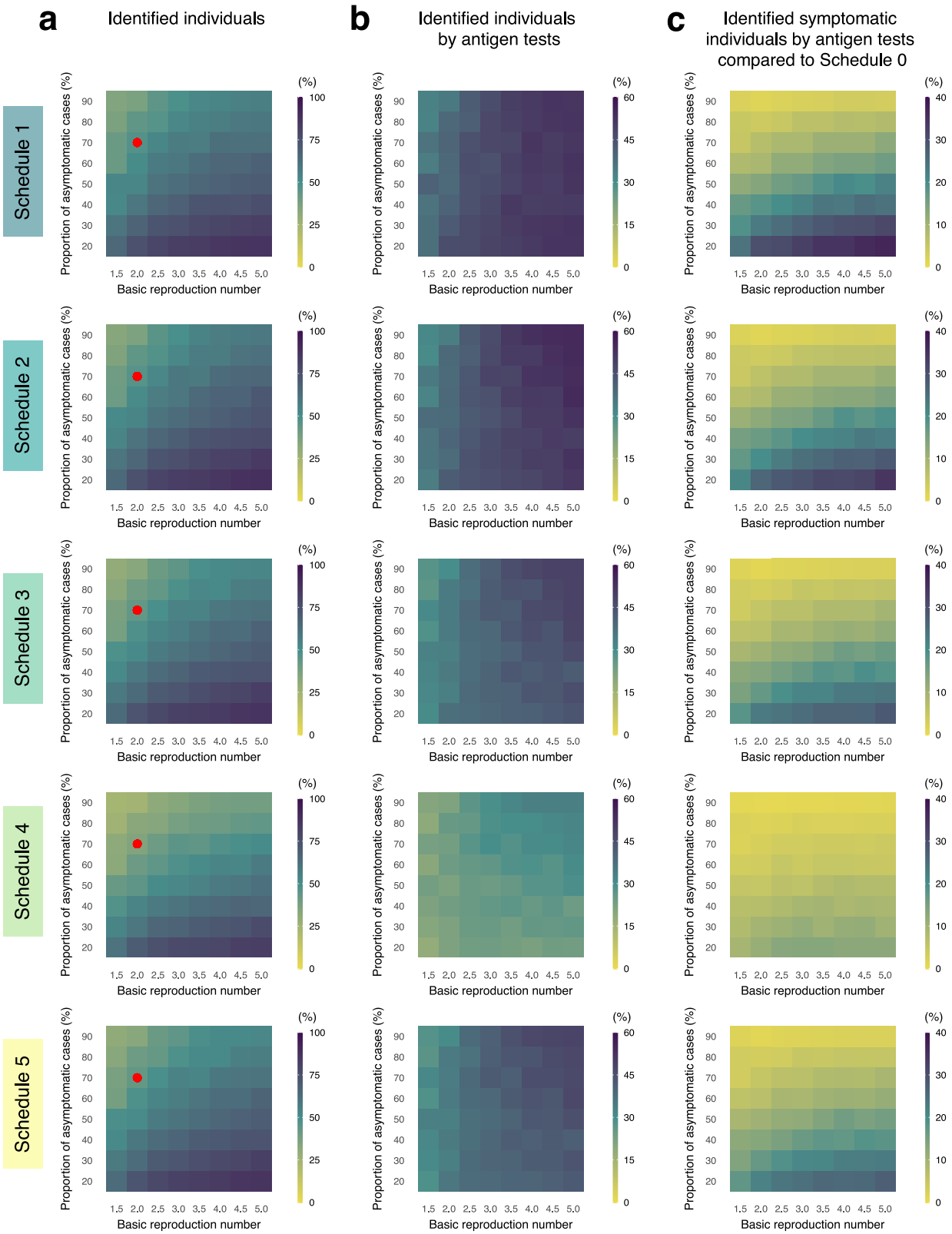

Fig. 5 | Effectiveness of different screening schedules on identifying SARS-CoV-2 infected individuals. Mean cumulative proportions of (**a**) identified SARS-CoV-2 infected individuals, (**b**) identified SARS-CoV-2 infected individuals by antigen tests, and (**c**) identified SARS-CoV-2 symptomatic individuals by antigen tests compared to Schedule 0 (third column panels) by the end of the screening programs under different screening schedules varying the proportion of asymptomatic cases and the basic reproduction number. Note that the different color scales in the three columns. Baseline parameter values for screening programs and those for the epidemic are used if not specified: $R_e = 2.0, p = 0.7$, low sensitivity tests [2.0×10^6 copies/mL], 10 days screening, screening initiation at peak phase, 4 antigen tests for each person. The red dots represent the baseline ($R_e = 2.0, p = 0.7$). Note that we did not count individuals infected during the screening period.

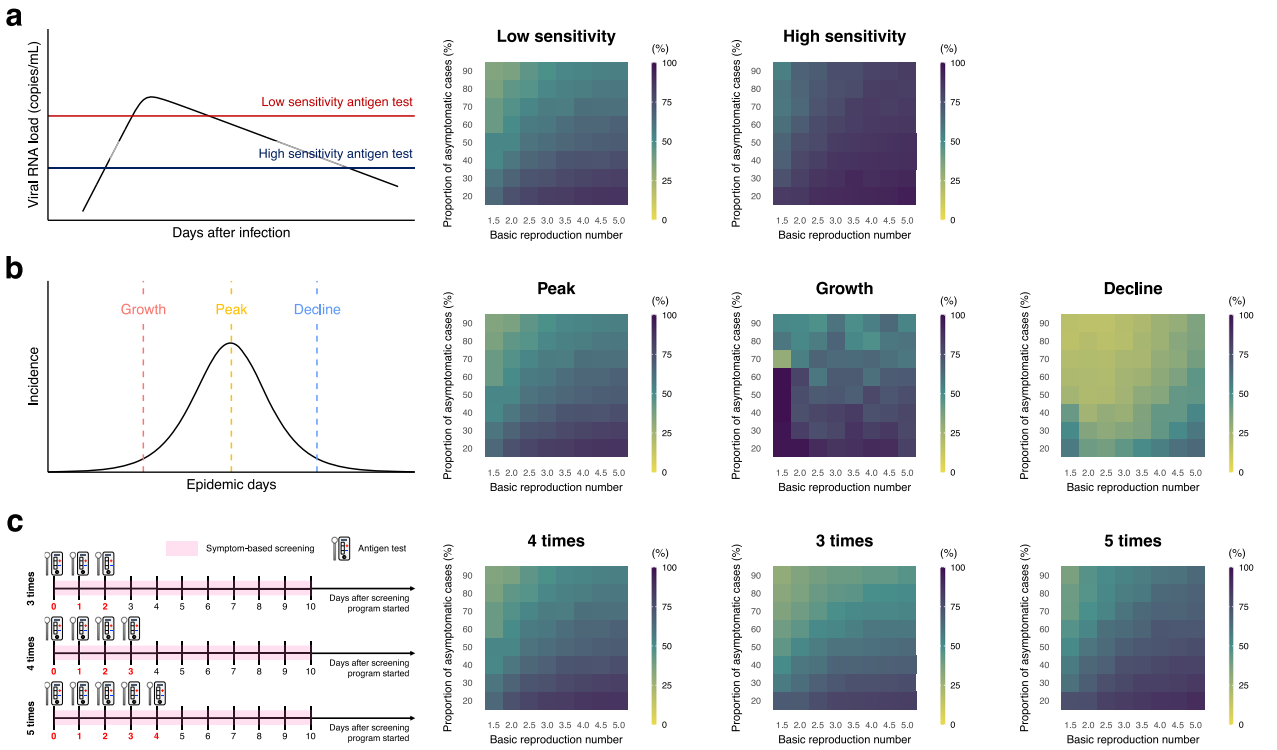

Fig. 6 | Effectiveness of different screening programs on identifying SARS-CoV-2 infected individuals varying parameters relevant to screening programs. Mean cumulative proportion of SARS-CoV-2 infected individuals by the end of screening programs **a**. with different antigen tests (i.e., low sensitivity tests [2.0×10^6 copies/mL] and high sensitivity tests [6.3×10^4 copies/mL]), **b**. with different timing of screening initiation (i.e., peak, growth, and decline phases), **c**. with different number of available antigen tests per person (i.e., 3, 4, and 5 times). Baseline parameter values for the screening program (i.e., low sensitivity tests [2.0×10^6 copies/mL], screening initiation at peak phase, 4 antigen tests for each person) were used if not specified.

model and chose parameter values to evaluate the effectiveness of screening programs as realistically as possible, there are a few limitations which could be addressed in future studies. First, we did not consider a false-positive rate of the antigen tests (specificity of antigen tests for SARS-CoV-2 has been estimated to be 99.6%[71]). If the false-positive rate is not negligible, targeted screening (targeting high prevalence populations) might also be an option to reduce the burden related to screening tests. Second, both the transmission model and the viral dynamics model did not consider emerging variants, reinfection, breakthrough infection, and vaccine effects. For example, if the viral dynamics of the delta variant or under vaccination is different from the original variant without vaccination (Li et al. suggested that the delta variant presented faster viral replication[72]), our model needs to be updated. However, our model is flexible enough to incorporate the effect of vaccination or variants into both the viral dynamics model and the transmission model once relevant data become available. Third, the transmission model did not incorporate behavioral changes during the pandemic or screening. Contact patterns dynamically changed as a response to the pandemic, which was partly responsible for the multiple waves of infection observed in most countries[73–75], and such behavioral dynamics could be incorporated into our modeling framework. Fourth, within-school/workplace transmission was assumed not to be influenced by the screening intervention. However, clusters of infections in school/workplace can take place even when interventions are implemented and the effective reproduction number is under the epidemic threshold[76–78]. Therefore, considering the possibility of transmission in the focus facility represents an important future direction of the current study. Fifth, the viral dynamics model used in this study is simple and did not incorporate additional factors such as the immune system. However, we believe that the adoption of the proposed minimal model is justified for the following reasons: i) our previous study[37] has shown that more complex models led to similar goodness of fit than the proposed model and the estimated distributions of model parameters were consistent between all models; and ii) more complex models require either fixing parameters or considering additional data that goes beyond longitudinal viral load (e.g., immunological response data), which would be challenging in the context of pandemic preparedness.

Our work has valuable scientific and public health implications. From the scientific standpoint, we have introduced a novel multi-scale approach to evaluate the efficacy of screening programs at the single facility level. Notably, the proposed viral dynamics model offers a more adaptable computational framework, enabling the simultaneous computation of epidemiological parameters and test sensitivity. From the public health standpoint, our computational framework can empower decision-makers to allocate resources more pragmatically. For example, in situations where resources are abundant, emphasis can be placed on deploying high-sensitivity tests and prioritizing early and frequent testing.

Regardless of the simplicity, we have proposed a computational framework to consider the effectiveness of various screening programs deployed at a small-scale, such as in schools and workplaces. Based on our analyses, for economic and educational activities to resume safely and in-person, we recommend frequent and early screening with high sensitivity antigen tests.

Data availability

The viral load data that support the findings of this study are publicly available, obtained from publications[35,36,46,79–86] (see Supplementary Table 2). Source data for the main figures are provided in the Supplementary Data file.

Code availability

The study's supporting codes are available at the Zenodo[58].

Received: 13 July 2023; Accepted: 17 December 2024;
Published online: 03 January 2025

References

1. Billah, M. A., Miah, M. M. & Khan, M. N. Reproductive number of coronavirus: a systematic review and meta-analysis based on global level evidence. *PLoS ONE* **15**, e0242128 (2020).
2. Zhen-Dong T. et al. Potential presymptomatic transmission of SARS-CoV-2, Zhejiang Province, China, 2020. *Emerging Infectious Dis. J.* **26**, 1052 (2020).
3. Kimball, A. et al. Asymptomatic and presymptomatic SARS-CoV-2 infections in residents of a long-term care skilled nursing facility—King County, Washington, March 2020. *MMWR Morb. Mortal. Wkly. Rep.* **69**, 377–381 (2020).
4. Arons, M. M. et al. Presymptomatic SARS-CoV-2 Infections and Transmission in a Skilled Nursing Facility. *N. Engl. J. Med.* **382**, 2081–2090 (2020).
5. Hu, S. et al. Infectivity, susceptibility, and risk factors associated with SARS-CoV-2 transmission under intensive contact tracing in Hunan, China. *Nat. Commun.* **12**, 1533 (2021).
6. Gupta, S. et al. Vaccinations against COVID-19 may have averted up to 140,000 deaths in the United States. *Health Aff.* **40**, 1465–1472 (2021).
7. Abu-Raddad, L. J., Chemaitelly, H. & Bertollini, R. Waning mRNA-1273 vaccine effectiveness against SARS-CoV-2 Infection in Qatar. *N. Engl. J. Med.* **386**, 1091–1093 (2022).
8. Andrews, N. et al. Covid-19 vaccine effectiveness against the Omicron (B.1.1.529) variant. *N. Engl. J. Med.* **386**, 1532–1546 (2022).
9. Fabiani, M. et al. Effectiveness of mRNA vaccines and waning of protection against SARS-CoV-2 infection and severe covid-19 during predominant circulation of the delta variant in Italy: retrospective cohort study. *BMJ* **376**, e069052 (2022).
10. Menni, C. et al. COVID-19 vaccine waning and effectiveness and side-effects of boosters: a prospective community study from the ZOE COVID Study. *Lancet Infectious Dis.* **22**, 1002–1010 (2022).
11. Feikin, D. R. et al. Duration of effectiveness of vaccines against SARS-CoV-2 infection and COVID-19 disease: results of a systematic review and meta-regression. *Lancet* **399**, 924–944 (2022).
12. Leung, K., Lau, E. H. Y., Wong, C. K. H., Leung, G. M. & Wu, J. T. Estimating the transmission dynamics of SARS-CoV-2 Omicron BF.7 in Beijing after adjustment of the zero-COVID policy in November-December 2022. *Nat. Med.* **29**, 579–582 (2023).
13. Xie, R. et al. Resurgence of Omicron BA.2 in SARS-CoV-2 infection-naive Hong Kong. *Nat. Commun.* **14**, 2422 (2023).
14. Betthauser, B. A., Bach-Mortensen, A. M. & Engzell, P. A systematic review and meta-analysis of the evidence on learning during the COVID-19 pandemic. *Nat. Hum. Behav.* **7**, 375–385 (2023).
15. Bird, K. A., Castleman, B. L. & Lohner, G. Negative impacts from the shift to online learning during the COVID-19 crisis: evidence from a statewide community college system. EdWorkingPaperscom (2020).
16. Huckins, J. F. et al. Mental health and behavior of college students during the early phases of the COVID-19 pandemic: longitudinal smartphone and ecological momentary assessment study. *J. Med. Internet Res.* **22**, e20185 (2020).
17. Li, H. Y., Cao, H., Leung, D. Y. P.& Mak, Y. W. The psychological impacts of a COVID-19 outbreak on college students in China: a longitudinal study. *Int. J. Environ. Res. Public Health* **17**, 3933 (2020).
18. Wang, C. et al. Immediate Psychological Responses and Associated Factors during the Initial Stage of the 2019 Coronavirus Disease (COVID-19) Epidemic among the General Population in China. *Int. J. Environ. Res. Public Health* **17**, 1729 (2020).
19. Sahu, P. Closure of universities due to coronavirus disease 2019 (COVID-19): impact on education and mental health of students and academic staff. *Cureus* **12**, e7541 (2020).
20. Toscano, F. & Zappalà, S. Social isolation and stress as predictors of productivity perception and remote work satisfaction during the COVID-19 pandemic: the role of concern about the virus in a moderated double mediation. *Sustainability* **12**, 9804 (2020).
21. Baudot, L. & Kelly, K. A survey of perceptions of remote work and work productivity in the United States during the COVID-19 shutdown. Available at SSRN 3646406 (2020).
22. Bartik, A. W., Cullen, Z. B., Glaeser, E. L., Luca, M. & Stanton, C. T. *What Jobs are Being Done at Home During the Covid-19 Crisis? Evidence from Firm-Level Surveys*. National Bureau of Economic Research Working Paper Series. No. 27422 (2020).
23. Galanti, T., Guidetti, G., Mazzei, E., Zappalà, S. & Toscano, F. Work from home during the COVID-19 outbreak: the impact on employees' remote work productivity, engagement, and stress. *J. Occup. Environ. Med.* **63**, e426–e432 (2021).
24. Lessler, J. et al. Household COVID-19 risk and in-person schooling. *Science* **372**, 1092–1097 (2021).
25. Leng, T. et al. Quantifying pupil-to-pupil SARS-CoV-2 transmission and the impact of lateral flow testing in English secondary schools. *Nat. Commun.* **13**, 1106 (2022).
26. Leng, T. et al. Assessing the impact of lateral flow testing strategies on within-school SARS-CoV-2 transmission and absences: a modelling study. *PLoS Comput. Biol.* **18**, e1010158 (2022).
27. Chen, X. et al. Estimation of disease burden and clinical severity of COVID-19 caused by Omicron BA.2 in Shanghai, February-June 2022. *Emerg. Microbes Infect.* **11**, 2800–2807 (2022).
28. Poletti, P. et al. Association of age with likelihood of developing symptoms and critical disease among close contacts exposed to patients with confirmed SARS-CoV-2 infection in Italy. *JAMA Netw. Open.* **4**, e211085 (2021).
29. Cohen, C. et al. SARS-CoV-2 incidence, transmission, and reinfection in a rural and an urban setting: results of the PHIRST-C cohort study, South Africa, 2020-21. *Lancet Infect. Dis.* **22**, 821–834 (2022).
30. He, X. et al. Temporal dynamics in viral shedding and transmissibility of COVID-19. *Nat. Med.* **26**, 672–675 (2020).
31. Lovell-Read, F. A., Funk, S., Obolski, U., Donnelly, C. A. & Thompson, R. N. Interventions targeting non-symptomatic cases can be important to prevent local outbreaks: SARS-CoV-2 as a case study. *J. R. Soc. Interface* **18**, 20201014 (2021).
32. Larremore, D. B. et al. Test sensitivity is secondary to frequency and turnaround time for COVID-19 screening. *Sci. Adv.* **7**, eabd5393 (2021).
33. Chen, Z. et al. Epidemiological characteristics and transmission dynamics of the outbreak caused by the SARS-CoV-2 Omicron variant in Shanghai China: a descriptive study. *Lancet Reg. Health West Pac.* **29**, 100592 (2022).
34. Liu, Q. H. et al. Model-based evaluation of alternative reactive class closure strategies against COVID-19. *Nat. Commun.* **13**, 322 (2022).
35. Peiris, J. S. M. et al. Clinical progression and viral load in a community outbreak of coronavirus-associated SARS pneumonia: a prospective study. *Lancet* **361**, 1767–1772 (2003).
36. Zou, L. et al. SARS-CoV-2 viral load in upper respiratory specimens of infected patients. *N. Engl. J. Med.* **382**, 1177–1179 (2020).
37. Jeong, Y. D. et al. Revisiting the guidelines for ending isolation for COVID-19 patients. *eLife* **10**, e69340 (2021).
38. Ejima, K. et al. Estimation of the incubation period of COVID-19 using viral load data. *Epidemics* **35**, 100454 (2021).
39. Ejima, K. et al. Time variation in the probability of failing to detect a case of polymerase chain reaction testing for SARS-CoV-2 as estimated from a viral dynamics model. *J. R. Soc. Interface* **18**, 20200947 (2021).
40. Kim, K. S. et al. A quantitative model used to compare within-host SARS-CoV−2, MERS-CoV, and SARS-CoV dynamics provides insights into the pathogenesis and treatment of SARS-CoV-2. *PLoS Biol.* **19**, e3001128 (2021).
41. Iwanami, S. et al. Detection of significant antiviral drug effects on COVID-19 with reasonable sample sizes in randomized controlled trials: a modeling study. *PLoS Med.* **18**, e1003660 (2021).
42. Goyal, A., Cardozo-Ojeda, E. F. & Schiffer, J. T. Potency and timing of antiviral therapy as determinants of duration of SARS-CoV-2

shedding and intensity of inflammatory response. *Sci. Adv.* **6**, eabc7112 (2020).
43. Gonçalves, A. et al. Timing of antiviral treatment initiation is critical to reduce SARS-CoV-2 viral load. *CPT Pharmacomet. Syst. Pharmacol.* **9**, 509–514 (2020).
44. Best, K. et al. Zika plasma viral dynamics in nonhuman primates provides insights into early infection and antiviral strategies. *Proc. Natl Acad. Sci. Usa.* **114**, 8847–8852 (2017).
45. Jeong, Y. D. et al. Designing isolation guidelines for COVID-19 patients with rapid antigen tests. *Nat. Commun.* **13**, 4910 (2022).
46. Wölfel, R. et al. Virological assessment of hospitalized patients with COVID-2019. *Nature* **581**, 465–469 (2020).
47. van Kampen, J. J. et al. Duration and key determinants of infectious virus shedding in hospitalized patients with coronavirus disease-2019 (COVID-19). *Nat. Commun.* **12**, 1–6 (2021).
48. Marc, A. et al. Quantifying the relationship between SARS-CoV-2 viral load and infectiousness. *medRxiv* https://doi.org/10.1101/2021.05.07.21256341 (2021).
49. Goyal, A., Reeves, D. B., Cardozo-Ojeda, E. F., Schiffer, J. T. & Mayer, B. T. Viral load and contact heterogeneity predict SARS-CoV-2 transmission and super-spreading events. *Elife* **10**, e63537 (2021).
50. Centers for Disease Control and Prevention. COVID Data Tracker 2021. Available from https://covid.cdc.gov/covid-data-tracker/.
51. Liu, Y., Gayle, A. A., Wilder-Smith, A. & Rocklov, J. The reproductive number of COVID-19 is higher compared to SARS coronavirus. *J. Travel Med.* **27**, taaa021 (2020).
52. Park, M., Cook, A. R., Lim, J. T., Sun, Y. & Dickens, B. L. A systematic review of COVID-19 epidemiology based on current evidence. *J. Clin. Med.* **9**, 967 (2020).
53. Dehning, J. et al. Inferring change points in the spread of COVID-19 reveals the effectiveness of interventions. *Science* **369**, eabb9789 (2020).
54. Yamaoka, Y. et al. Highly specific monoclonal antibodies and epitope identification against SARS-CoV-2 nucleocapsid protein for antigen detection tests. *Cell Rep. Med.* **2**, 100311 (2021).
55. Reddy, K. P. et al. Clinical outcomes and cost-effectiveness of COVID-19 vaccination in South Africa. *Nat. Commun.* **12**, 6238 (2021).
56. Reddy, K. P. et al. Cost-effectiveness of public health strategies for COVID-19 epidemic control in South Africa: a microsimulation modelling study. Lancet. *Glob. Health* **9**, e120–e129 (2021).
57. Du, Z., Pandey, A., Bai, Y., Fitzpatrick, M. C. & Chinazzi, M. et al. Comparative cost-effectiveness of SARS-CoV-2 testing strategies in the USA: a modelling study. *Lancet Public Health* **6**, e184–e191 (2021).
58. Jeong, Y. D. Safe return to schools and workplaces: a modelling study to define guidelines for antigen screening in schools and workplaces to mitigate COVID-19 outbreaks 2023. Available from https://doi.org/10.5281/zenodo.8041485.
59. Centers for Disease Control and Prevention (CDC). Information for Pediatric Healthcare Providers 2024. Available from https://www.cdc.gov/coronavirus/2019-ncov/hcp/pediatric-hcp.html.
60. Costa, R. et al. Upper respiratory tract SARS-CoV-2 RNA loads in symptomatic and asymptomatic children and adults. *Clin. Microbiol. Infect.* **27**, 1858 e1–e7 (2021).
61. Cevik, M., Tate, M., Lloyd, O., Maraolo, A. E. & Schafers, J. Ho A. SARS-CoV-2, SARS-CoV, and MERS-CoV viral load dynamics, duration of viral shedding, and infectiousness: a systematic review and meta-analysis. *Lancet Microbe* **2**, e13–e22 (2021).
62. Pavelka, M. et al. The impact of population-wide rapid antigen testing on SARS-CoV-2 prevalence in Slovakia. *Science* **372**, 635–641 (2021).
63. Hellewell, J. et al. Estimating the effectiveness of routine asymptomatic PCR testing at different frequencies for the detection of SARS-CoV-2 infections. *BMC Med.* **19**, 106 (2021).
64. Hart, W. S. et al. Analysis of the risk and pre-emptive control of viral outbreaks accounting for within-host dynamics: SARS-CoV-2 as a case study. *Proc. Natl Acad. Sci.* **120**, e2305451120 (2023).
65. Sunagawa, J. et al. Isolation may select for earlier and higher peak viral load but shorter duration in SARS-CoV-2 evolution. *Nat. Commun.* **14**, 7395 (2023).
66. Jones, T. C. et al. Estimating infectiousness throughout SARS-CoV-2 infection course. *Science* **373**, eabi5273 (2021).
67. van Kampen, J. J. A. et al. Duration and key determinants of infectious virus shedding in hospitalized patients with coronavirus disease-2019 (COVID-19). *Nat. Commun.* **12**, 267 (2021).
68. Ke, R. et al. Daily longitudinal sampling of SARS-CoV-2 infection reveals substantial heterogeneity in infectiousness. *Nat. Microbiol.* **7**, 640–652 (2022).
69. Singanayagam, A. et al. Duration of infectiousness and correlation with RT-PCR cycle threshold values in cases of COVID-19, England, January to May 2020. *Eurosurveillance* **25**, 2001483 (2020).
70. Marc, A. et al. Quantifying the relationship between SARS-CoV-2 viral load and infectiousness. *Elife* **10**, e69302 (2021).
71. Dinnes, J. et al. Rapid, point-of-care antigen and molecular-based tests for diagnosis of SARS-CoV-2 infection. *Cochrane Database Syst. Rev*. **8**, CD013705 (2021).
72. Li, B. et al. Viral infection and transmission in a large, well-traced outbreak caused by the SARS-CoV-2 Delta variant. *Nat. Commun*. **13**, **460** (2021).
73. Feehan, D. M. & Mahmud, A. S. Quantifying population contact patterns in the United States during the COVID-19 pandemic. *Nat. Commun.* **12**, 893 (2021).
74. Crane, M. A., Shermock, K. M., Omer, S. B. & Romley, J. A. Change in reported adherence to nonpharmaceutical interventions during the COVID-19 pandemic, April-November 2020. *JAMA* **325**, 883–885 (2021).
75. Zhang, J. et al. Changes in contact patterns shape the dynamics of the COVID-19 outbreak in China. *Science* **368**, 1481–1486 (2020).
76. Shaw, C. L. & Kennedy, D. A. What the reproductive number R(0) can and cannot tell us about COVID-19 dynamics. *Theor. Popul Biol.* **137**, 2–9 (2021).
77. Molina Grane, C. et al. SARS-CoV-2 transmission patterns in educational settings during the Alpha wave in Reggio-Emilia. *Italy Epidemics.* **44**, 100712 (2023).
78. Manica, M. et al. Estimating SARS-CoV-2 transmission in educational settings: A retrospective cohort study. *Influenza Other Respir. Viruses.* **17**, e13049 (2023).
79. Kissler, S. M. et al. Densely sampled viral trajectories for SARS-CoV-2 variants alpha (B. 1.1. 7) and epsilon (B. 1.429). *medRxiv* https://doi.org/10.1101/2021.02.16.21251535 (2021).
80. Kissler Stephen, M. et al. Sars-cov-2 viral dynamics in acute infections. *medRxiv* https://doi.org/10.1101/2020.10.21.20217042 (2020).
81. Jang, S., Rhee, J. Y., Wi, Y. M. & Jung, B. K. Viral kinetics of SARS-CoV-2 over the preclinical, clinical, and postclinical period. *Int J. Infect. Dis.* **102**, 561–565 (2021).
82. Kim, E. S. et al. Clinical course and outcomes of patients with severe acute respiratory syndrome coronavirus 2 infection: a preliminary report of the first 28 patients from the Korean Cohort Study on COVID-19. *J. Korean Med Sci.* **35**, e142 (2020).
83. Young, B. E. et al. Epidemiologic features and clinical course of patients infected with SARS-CoV-2 in Singapore. *JAMA* **323**, 1488–1494 (2020).
84. Sakurai, A. et al. Natural history of asymptomatic SARS-CoV-2 infection. *N. Engl. J. Med.* **383**, 885–886 (2020).
85. Kim, S. E. et al. Viral kinetics of SARS-CoV-2 in asymptomatic carriers and presymptomatic patients. *Int J. Infect. Dis.* **95**, 441–443 (2020).
86. Kam, K. Q. et al. SARS-CoV-2 viral RNA load dynamics in the nasopharynx of infected children. *Epidemiol. Infect.* **149**, e18 (2021).

Acknowledgements

The authors would like to thank Yoshihiro Okada, Junichi Katada, Atsuhiko Wada, Kaku Irisawa and Toshiki Takei at Fujifilm Corporation for useful discussion. This study was supported in part by Basic Science Research Program through the National Research Foundation of Korea grant RS-2024-00345478 (to Y.D.J), 2022R1C1C2003637 (to K.S.K.), and 2022R1A5A1033624 (to I.H.J); Grants-in-Aid for JSPS Scientific Research (KAKENHI) B18KT0018 (to S.Iwami.), 18H01139 (to S.Iwami.), 16H04845 (to S.Iwami.), Scientific Research in Innovative Areas 20H05042 (to S.Iwami.); AMED Strategic International Brain Science Research Promotion Program (to K.A.); AMED CREST 19gm1310002 (to S.Iwami.); AMED Japan Program for Infectious Diseases Research and Infrastructure, 20wm0325007h0001 (to S.Iwami.), 20wm0325004s0201 (to S.Iwami.), 20wm0325012s0301 (to S.Iwami.), 20wm0325015s0301 (to S.Iwami.); AMED Research Program on HIV/AIDS 19fk0410023s0101 (to S.Iwami.); AMED Research Program on Emerging and Re-emerging Infectious Diseases 19fk0108050h0003 (to S.Iwami.), 19fk0108156h0001 (to S.Iwmai.), 20fk0108140s0801 (to S.Iwami.) and 20fk0108413s0301 (to S.Iwami.); AMED Program for Basic and Clinical Research on Hepatitis 19fk0210036h0502 (to S.Iwami.); AMED Program on the Innovative Development and the Application of New Drugs for Hepatitis B 19fk0310114h0103 (to S.Iwami.); JST MIRAI (to S.Iwami.); Moonshot R&D Grant Number JPMJMS2021 (to K.A. and S.Iwami.) and JPMJMS2025 (to S.Iwami.); Mitsui Life Social Welfare Foundation (to S.Iwami.); Shin-Nihon of Advanced Medical Research (to S.Iwami.); Suzuken Memorial Foundation (to S.Iwami.); Life Science Foundation of Japan (to S.Iwami.); SECOM Science and Technology Foundation (to S.Iwami.); The Japan Prize Foundation (to S.Iwami.); Daiwa Securities Health Foundation (to S.Iwami.); the MIDAS Coordination Center (MIDASSUGP2020-6) by a grant from the National Institute of General Medical Science (3U24GM132013-02S2) (to K.E.); a Lee Kong Chian School of Medicine startup grant (LKCMedicine-SUG, #022388-00001) (to K.E.); JST, PRESTO (JPMJPR23R3) (to K.E.); Fujifilm Corporation (to K.E. and S.Iwami); JST, PRESTO (JPMJPR23R3). M.A. acknowledges funding from the Cooperative Agreement number NU38OT000297 from the Centers for Disease Control and Prevention (CDC) and the Council of State and Territorial Epidemiologists (CSTE). The study does not necessarily represent the views of CDC and CSTE. The funders had no role in the design and conduct of the study; collection, management, analysis, and interpretation of the data; preparation, review, or approval of the manuscript; and decision to submit the manuscript for publication.

Author contributions

K.E., S.Iwami, and K.A. designed the research. Y.D.J., K.E., K.S.K., S.I., and S.Iwami carried out the computational analysis. K.E. and S.Iwami supervised the project. Y.D.J., K.E., K.S.K., S.I., W.S.H., R.N.T., I.H.J., S.Iwami, M.A., and K.A. contributed to writing the manuscript.

Competing interests

M.A. has received research funding from Seqirus. The funding is not related to the current research. K.E. and S.Iwami received funding from Fujifilm Corporation, which produces and sells SARS-CoV-2 antigen rapid diagnostic tests. However, this competing interest did not influence the design, execution, or interpretation of the study. The authors declare that they have no other competing interests.

Additional information

Supplementary information The online version contains supplementary material available at https://doi.org/10.1038/s43856-024-00716-3.

Correspondence and requests for materials should be addressed to Keisuke Ejima or Shingo Iwami.

Peer review information *Communications Medicine* thanks Francisco Reche and the other, anonymous, reviewer(s) for their contribution to the peer review of this work.

Reprints and permissions information is available at http://www.nature.com/reprints

Publisher's note Springer Nature remains neutral with regard to jurisdictional claims in published maps and institutional affiliations.

Open Access This article is licensed under a Creative Commons Attribution-NonCommercial-NoDerivatives 4.0 International License, which permits any non-commercial use, sharing, distribution and reproduction in any medium or format, as long as you give appropriate credit to the original author(s) and the source, provide a link to the Creative Commons licence, and indicate if you modified the licensed material. You do not have permission under this licence to share adapted material derived from this article or parts of it. The images or other third party material in this article are included in the article's Creative Commons licence, unless indicated otherwise in a credit line to the material. If material is not included in the article's Creative Commons licence and your intended use is not permitted by statutory regulation or exceeds the permitted use, you will need to obtain permission directly from the copyright holder. To view a copy of this licence, visit http://creativecommons.org/licenses/by-nc-nd/4.0/.

© The Author(s) 2025

[1]Interdisciplinary Biology Laboratory (iBLab), Division of Biological Science, Graduate School of Science, Nagoya University, Nagoya, Japan. [2]Department of Mathematics, Pusan National University, Busan, South Korea. [3]Lee Kong Chian School of Medicine, Nanyang Technological University, Singapore, Singapore. [4]Department of Scientific Computing, Pukyong National University, Busan, South Korea. [5]Mathematical Institute, University of Oxford, Oxford, UK. [6]Mathematics Institute, University of Warwick, Coventry, UK. [7]Finace Fishery Manufacture Industrial Mathematics Center on Big Data, Pusan National University, Busan, South Korea. [8]Institute of Mathematics for Industry, Kyushu University, Fukuoka, Japan. [9]Institute for the Advanced Study of Human Biology (ASHBi), Kyoto University, Kyoto, Japan. [10]NEXT-Ganken Program, Japanese Foundation for Cancer Research (JFCR), Tokyo, Japan. [11]Science Groove Inc., Fukuoka, Japan. [12]Laboratory for Computational Epidemiology and Public Health Department of Epidemiology and Biostatistics, Indiana University School of Public Health-, Bloomington, IN, USA. [13]International Research Center for Neurointelligence, The University of Tokyo, Tokyo, Japan. [14]These authors contributed equally: Yong Dam Jeong, Keisuke Ejima, Kwang Su Kim. [15]These authors jointly supervised this work: Marco Ajelli, Kazuyuki Aihara. ✉e-mail: keisuke.ejima@ntu.edu.sg; iwami.iblab@bio.nagoya-u.ac.jp